



ACOUSTICS 2012

Towards a steelpan making model - Residual stress field effects on dynamical properties

M. Monteil^{a,b}, O. Thomas^c, J. Frelat^a, C. Touzé^b and W. Seiler^d

^aIJLRDA-UPMC, 4 place jussieu, 75005 PARIS, France

^bUME (Unité de Mécanique), ENSTA - ParisTech, Chemin de la Hunière, 91761 Palaiseau, France

^cLMSSC-CNAM, 2 rue conté, 75003 PARIS, France

^dLaboratoire PIMM, Arts & Métiers Paristech, 151 boulevard de l'hôpital, 75013 Paris, France
melodie.monteil@gmail.com

This paper is devoted to modelize steelpan making, with the special emphases on the first step, which consists in sinking the drum head by hand with a pneumatic hammer. The main concern is to develop a model accounting for the large change of geometry encountered by the initial clamped circular plate, which is transformed in a spherical shell, and its influence on the vibratory properties of the structure. We propose here a simple one-dimensional model: a hinged-hinged beam, subjected to selected external static forces that deform it into a curved beam of profile close to the one of the top surface of the steelpan after the first making step. Several loadings, including axial force and/or bending moment, are considered, and the influence of the residual stress state on the eigenfrequencies of the final structures is quantitatively obtained.

1 Introduction

Steelpan belong to a musical instruments family coming from the island of Trinidad and Tobago. They are usually played in steelbands, that are orchestras composed of steelpans covering a range of several octaves. A steelpan is a tuned percussion, built from cylindrical steel barrels. The circular plate on the top is subjected to several stages of metal forming that stretch and bend the structure. Steelpan making consists in pressing, hammering, punching and burning in order to obtain a sort of main bowl within which convex substructures are formed. Each convex dome corresponds to a musical note where natural frequencies are precisely tuned according to harmonic relationships (f , $2f$, 3 (or 4) f , ...). Usually, this instrument is played by striking each note with a stick covered with a piece of rubber (Fig. 1).



Figure 1: Playing steelpan

Vibrations modelling have been proposed in a series of papers by Achong *et al.* [1, 2]. In these works, the steelpan is considered as a nonlinear system of oscillators, and energy transfers between normal modes of vibration are highlighted. Rossing *et al.* [11, 10] have performed modal analyses by holographic techniques to observe modal interactions between harmonically tuned notes. More recently, numerical modal analyses with the finite element methods have been proposed, accounting for the precise geometry of a tenor bass steelpan [4]. The steelpan's sound radiation has been recently addressed experimentally [7]. Finally, some metallurgical issues during the steelpan making have been considered in [8].

In all the previous literature works, the whole making process is not taken into account in the acoustic modelling and the steelpan is always considered as a vibrating structure free of residual stresses. The present study aims at filling this gap. During the making process, the initially flat circular plate at the top of the barrel is subjected to several deformations to progressively change its shape into the final one of the steelpan. The final state of the structure after those plastic deformations is characterized by a plastic strain field that leads to two components: (i) a *deformed geometry*, which is in equilibrium with (ii) a *particular residual stress field*.

Since only the final state of the structure is under concern, there is no need of computing all the successive plastic deformations steps (which would be a cumbersome operation). The main goal of the present work is to study the part of those two characteristics (the final geometry and the residual stresses) on the vibratory characteristics of the steelpan.

The present study focuses on the first step of the steelpan making, the sinking, in which the circular plate at the top of the barrel is transformed into an almost spherical shell. Only a simple one-dimensional model is considered, a hinged-hinged beam. Initially flat, it is subjected to axial tension and bending moments in order to give it a circular profile, with a center height close to 100 times the beam thickness. As a consequence, a geometrically nonlinear model of the beam is used as well as a numerical following path method to compute the final geometry. Then, the eigenfrequencies of the deformed and stressed beam are computed, and the influence of both the residual stress state and the deformed geometry are quantified.

2 Steelpan tuning and measurements

2.1 Deformation

A pneumatic hammer is used by the steelpan maker (the tuner) in order to progressively transform an initial barrel (Fig. 2) into a curved structure (Fig. 3). Initially, the diameter of the circular plate is $D = 567$ mm with a thickness $h = 1.3$ mm. The tuner controls regularly the depth of the center which finally reaches $H = 124$ mm. The whole process lasts around two hours.



Figure 2: Steel barrel typically used for steelpan making

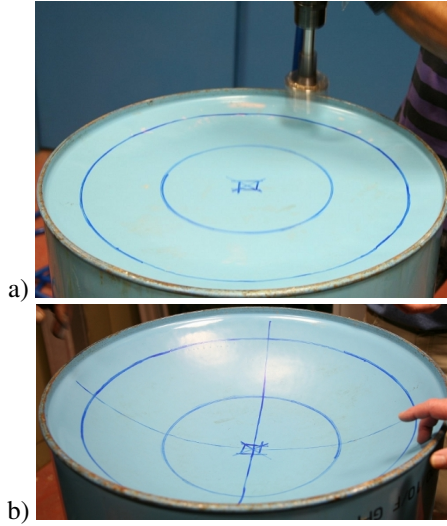


Figure 3: a) The top surface of the steelpan during pneumatic hammering ; b) Final spherical shell obtained after the process

2.2 Residual stress measurements

Measurement of the residual stresses have been realized at 8 points of the upper skin of the top shell of the barrel. Six points have been selected on a given radius, and two other points have been chosen on a different radius in order to check the axial symmetry (Fig. 4a). Measurements, realized thanks to a X-ray diffractometry [5], are reported on Fig. 4b. The measured residual stresses are positive, which means that tensile state is at hand. The order of magnitude is 10^8 Pa, and axisymmetry appears to be fairly well recovered.

3 Analytical one dimensional model

3.1 Prestressed beam model

In order to obtain the deformed geometry and study the effects of the residual stresses on the dynamic behaviour, an Euler-Bernoulli's beam of total length L , with a rectangular cross-section of width b and thickness h , is considered (Fig. 5). It is made of an homogeneous and isotropic material of Young's modulus E , Poisson ratio ν and density ρ . Hinged-hinged boundary conditions are imposed at $x = 0$ and $x = L$.

The classical constitutive law of the prestressed beam reduces to:

$$\sigma_{xx} = E\epsilon_{xx} - \sigma_{0xx}. \quad (1)$$

where σ_{xx} and ϵ_{xx} are the axial stress and strain. σ_{0xx} is an initial imposed stress used to model plastic strains imposed to the top plate of the barrel during the first making step.

A von Kármán model is used to express the strain/displacement relationship as $\epsilon_{xx} = u' + \frac{1}{2}w'^2 - zw''$ where u and w are the axial and transverse displacement, respectively, and $(.)' = \partial(.)/\partial x$.

From the local stress relation Eq. (1), the resultant axial

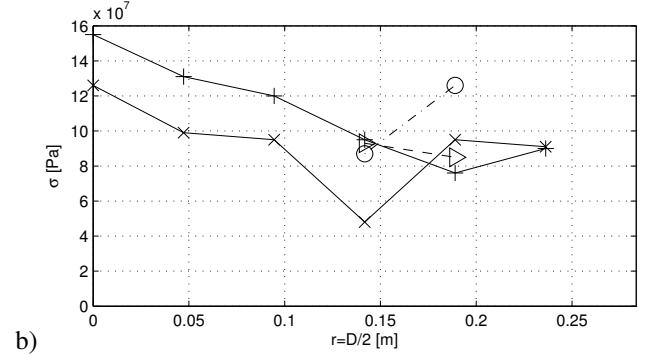
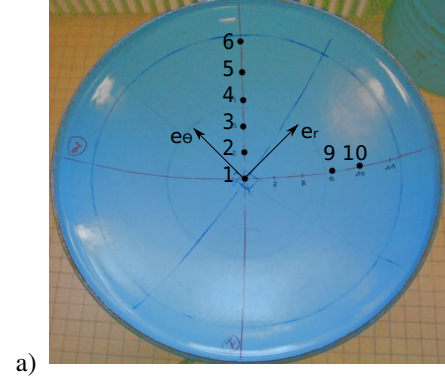


Figure 4: Surface stress measurement by X-ray diffractometry after sinking the barrel: on the points 1, 2, 3, 4, 5 and 6 (x) : $\sigma_{\theta\theta}$; (+) : σ_{rr} and on the points 9 and 10 (o) : $\sigma_{\theta\theta}$; (p) : σ_{rr}

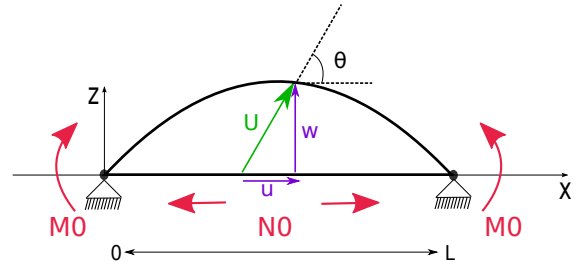


Figure 5: Hinged-hinged prestressed buckled beam

force and bending moment are:

$$\begin{cases} N = \iint_S \sigma dS = ES(u' + \frac{1}{2}w'^2) - N_0, \\ M = \iint_S z\sigma dS = EIw'' - M_0. \end{cases} \quad (2)$$

where $S = bh$ and $I = bh^3/12$. The initial load σ_{0xx} now appears as an initial imposed axial force, $N_0 = \iint_S \sigma_{0xx} dS$ and an initial bending moment $M_0 = \iint_S z\sigma_{0xx} dS$.

The equations of motion for the displacement of the beams read [9]:

$$\begin{cases} \rho S \ddot{w} + EIw'''' - (Nw')' + M_0'' = 0 \\ \rho S \ddot{u} - N' = 0 \end{cases} \quad (3)$$

Neglecting axial inertia implies $N' = 0$ so that N is uniform in $[0, L]$ and:

$$\int_0^L N dx = LN = \frac{ES}{2} \int_0^L w'^2 dx - LN_0 \quad (4)$$

where $\bar{N}_0 = \frac{1}{L} \int_0^L N_0 dx$ is the mean value of the imposed axial stress N_0 .

Those equations are made dimensionless by introducing:

$$\bar{w} = w/h \quad , \quad \bar{x} = x/L \quad (5)$$

and

$$\bar{t} = \frac{1}{L^2} \sqrt{\frac{EI}{\rho S}} t \quad , \quad \bar{N} = N \frac{L^2}{ES h^2} \quad \text{and} \quad \bar{M} = M \frac{L^2}{EI h} \quad (6)$$

so that, the nondimensional problem to solve finally reads (where bars are omitted for the sake of clarity):

$$\begin{cases} \ddot{w} + w'''' - \varepsilon N w'' - M'' = 0 & (7a) \\ N = \frac{1}{2} \int_0^1 w'^2 dx - \bar{N}_0 & (7b) \end{cases}$$

where $\varepsilon = \frac{S w_0^2}{T}$ is a nondimensional nonlinear coupling parameter.

It should be noticed that the x -dependance of the axial initial force N_0 has no influence on the model which depends only of its mean value \bar{N}_0 .

3.2 Static and dynamical problems

By imposing increasing values of \bar{N}_0 and M_0 , the beam will buckle and reach an equilibrium state. Our goal is twofold: first to find a couple of initial structural stress field (\bar{N}_0, M_0) allowing to reach the measured shape of the steelpan at the end of the process ; second, to investigate the vibrations around this buckled state. The influence of the residual stress state and geometry on the eigenfrequencies will be quantified.

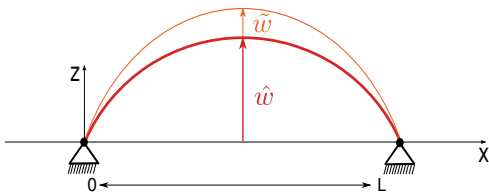


Figure 6: Static and dynamical problems: vibration around an equilibrium buckled state

The transverse displacement and internal axial force are separated in a static part (\hat{w}, \hat{N}) and a dynamical one (\tilde{w}, \tilde{N}) as:

$$\begin{cases} w(x, t) = \hat{w}(x) + \tilde{w}(x, t), \\ N(x, t) = \hat{N}(x) + \tilde{N}(x, t). \end{cases} \quad (8)$$

Introducing (8) into (7) we obtain the following static problem:

$$\begin{cases} \hat{w}'''' - \varepsilon \hat{N} \hat{w}'' - M_0'' = 0, & (9a) \\ \hat{N} = \frac{1}{2} \int_0^1 \hat{w}'^2 dx - \bar{N}_0. & (9b) \end{cases}$$

and the dynamical one:

$$\begin{cases} \ddot{\tilde{w}} + \tilde{w}'''' - \varepsilon \hat{N} \tilde{w}'' - \varepsilon \tilde{N} \hat{w}'' - \varepsilon \tilde{N} \tilde{w}'' = 0, & (10a) \\ \tilde{N} = \frac{1}{2} \int_0^1 \tilde{w}'^2 dx + \int_0^1 \tilde{w}' \hat{w}' dx. & (10b) \end{cases}$$

Finally, by neglecting all nonlinear dynamical terms in Eqs. (10a,b), the linear vibration \tilde{w} of the structure around the prestressed deformed state \hat{w} are solutions of:

$$\ddot{\tilde{w}} + \tilde{w}'''' - \underbrace{\varepsilon \hat{N} \tilde{w}''}_{\text{residual stress}} - \underbrace{\varepsilon \hat{w}'' \int_0^1 \tilde{w}' \hat{w}' dx}_{\text{geometry}} = 0 \quad (11)$$

Equation (11) represents the linear vibration of a straight beam, modified by two additional terms: one associated to the residual stresses \hat{N} and one related to the static deformed geometry of the beam \hat{w} .

3.3 Discretisation

The two problems are discretised by expanding the unknowns on the linear modes basis $\{\Phi_k\}$ of the unbuckled problem without prestress:

$$\hat{w}(x) = \sum_{k=1}^K \Phi_k(x) \hat{q}_k \quad \text{and} \quad \tilde{w}(x, t) = \sum_{k=1}^K \Phi_k(x) \tilde{q}_k(t) \quad (12)$$

where q_k is the modal coordinate and $\Phi_k = \sqrt{2} \sin(k\pi x)$ is the normalised mode shape ($\int_0^L \Phi_k^2(x) dx = 1$) for the hinged-hinged beam, solution of the linear problem $\Phi_k'''' - \omega_k^2 \Phi_k = 0$, with ω_k , the corresponding natural frequency.

3.3.1 Static problem

Introducing Eq. (12) into Eq. (9), multiplying the result by Φ_k , integrating over the length of the beam and using the orthogonality properties of the modes leads to the following problem for the unknowns $\{\hat{q}_k\}_{k=1 \dots K}$:

$$\begin{cases} \omega_k^2 \hat{q}_k + \varepsilon \hat{N} \sum_{i=1}^K \alpha_i^k \hat{q}_i - K_0^k = 0, & (13a) \end{cases}$$

$$\begin{cases} \hat{N} = \frac{1}{2} \sum_{i=1}^K \sum_{k=1}^K \alpha_i^k \hat{q}_i \hat{q}_k - \bar{N}_0. & (13b) \end{cases}$$

where, according to the boundary conditions,

$$\alpha_i^k = - \int_0^1 \Phi_k'' \Phi_i dx = \int_0^1 \Phi_i' \Phi_k' dx \text{ is a nonlinear coupling coefficient.}$$

In Eq. (13a) we observe that the initial stress field appears through \bar{N}_0 and $K_0^k = \int_0^1 M_0'' \Phi_k dx$.

We will see in section 4 that a simple uniform distribution of bending moment ($M_0(x) = M_0 \forall x$), associated to an axial force \bar{N}_0 , is sufficient to create a static deformation to the beam very close to the one measured on the deformed upper surface of the steelpan shown in Fig. 3(b) after the first making step. The corresponding value of K_0^k , computed with $M_0(x) = M_0[H(x) - H(x-1)]$, is $K_0^k = -2\sqrt{2}M_0k\pi$ if k is even, and zero if k is odd. One can notice that this uniform distribution of bending moment is equivalent to two concentrated moments applied at the beam's ends, $x = 0$ and $x = 1$.

3.3.2 Dynamical problem of the prestressed beam

Modal expansion for Eq. (11) leads to the dynamical problem expressed with the modal unknowns $\{\tilde{q}_k\}_{k=1\dots K}$:

$$\ddot{\tilde{q}}_k + \omega_k^2 \tilde{q}_k + \varepsilon \left(\underbrace{\hat{N} \sum_{i=1}^K \alpha_i^k \tilde{q}_i}_{\text{residual stress}} + \underbrace{\sum_{i,j,l=1}^K \alpha_i^l \alpha_j^k \tilde{q}_j \hat{q}_l \hat{q}_i}_{\text{geometry}} \right) = 0 \quad (14)$$

This dynamical problem allows to study linear vibrations around the buckled equilibrium state.

Eq. (14) can be written in matrix formulation as $\ddot{\tilde{\mathbf{q}}} + \mathbf{A}\tilde{\mathbf{q}} = \mathbf{0}$, with

$$A_{ki} = \omega_k^2 \delta_{ki} + \varepsilon \left(\underbrace{-\bar{N}_0 \alpha_i^k + \frac{1}{2} \sum_{j,l=1}^K \alpha_i^k \alpha_j^l \hat{q}_j \hat{q}_l}_{\text{residual stress}} + \underbrace{\sum_{j,l=1}^K \alpha_j^k \alpha_l^i \hat{q}_j \hat{q}_l}_{\text{geometry}} \right) \quad (15)$$

The eigenfrequencies of the dynamical problem (vibrations around the buckled state) are finally given by diagonalizing \mathbf{A} .

Eq. (15) shows that two different kinds of added terms have an influence on matrix \mathbf{A} (and thus on the eigenfrequencies): those arising from the residual stress state \hat{N} , and those from the deformed geometry \hat{w} . The influence of the residual stress on the eigenfrequencies can thus be quantified by comparing the eigenvalues of \mathbf{A} computed with ($\hat{N} \neq 0$) or without ($\hat{N} = 0$) the corresponding term.

4 Numerical results and discussion

The static problem Eq. (13) is an algebraic equation for the unknowns $\{\hat{q}_k\}_{k=1\dots K}$ depending on two parameters (\bar{N}_0 , M_0). It is solved by a continuation method, implemented in the software MANLAB, based on the asymptotic-numerical method [3, 6]. The continuation procedure imposes the choice of a control parameter λ linked to the initial stresses. We then replace in the computation algorithm \bar{N}_0 by $\lambda \bar{N}_0$ and M_0 by λM_0 , so that increasing λ leads to increase M_0 and N_0 in the same proportion.

In the aim of comparing numerical results to the experimental measurements, we use dimensioned variables. For this, value of classical steel parameters, as $\rho = 7500 \text{ kg/m}^3$ and $E = 210 \text{ MPa}$, are used. Also, we consider a beam with a total length $L = D = 567 \text{ mm}$, a thickness $h = 1.3 \text{ mm}$, and the maximal amplitude of \hat{w} as $\hat{w}(L/2) \approx 124 \text{ mm}$.

Two different cases are investigated, shown in Fig 7a. First, we show a classical buckled state related to a pure axial loading ($\bar{N}_0 \neq 0$ and $M_0 = 0$). We can notice that the resulting deflection does not fit perfectly the measured shape of the steelpan. Then, we add a bending moment ($\bar{N}_0 \neq 0$ and $M_0 \neq 0$) in order to increase the curvature near the boundaries. We observe that, for $\bar{N}_0 = 30930$ and $M_0 = 3093$, the buckled state perfectly fit the measured profile.

Figure 7(b) shows the two corresponding buckling diagrams.

We can see that in the first case, a perfect pitchfork bifurcation is observed (only one solution branch has been reported in the figure). When $M_0 \neq 0$ a degenerate bifurcation is at hand.

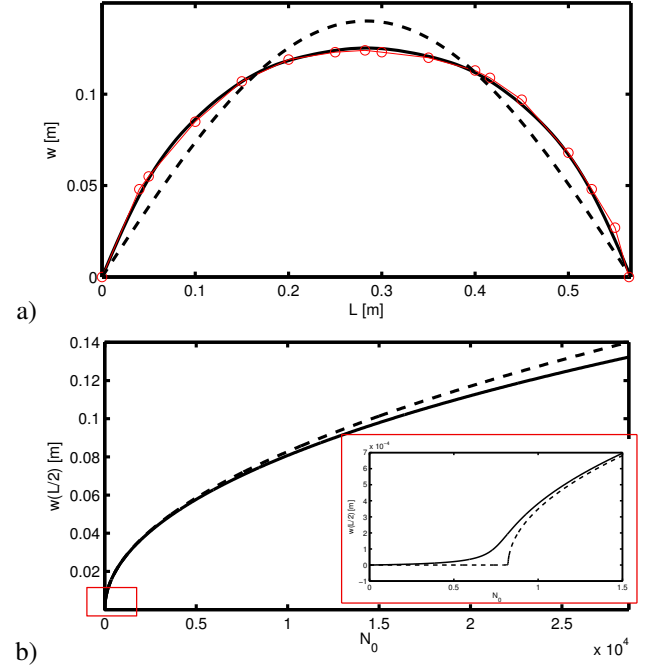


Figure 7: Static solutions: (---) $\bar{N}_0 \neq 0$, $M_0 = 0$; (—) \bar{N}_0 and $M_0 \neq 0$ (a) numerical results \hat{w} compared with the experimental profile $\circ - \circ$; (b) corresponding buckling diagram for $\hat{w}_{max} = \hat{w}(L/2)$

Figure 8 presents the evolution of the mean value of the local residual stress $\sigma = \hat{N}/S$ (with $S = bh$ the cross-section area of the beam) as a function of \bar{N}_0 . In both cases, σ decreases until the buckling load ($\bar{N}_0 = \bar{N}_{0c}$) is reached. When there is no added bending moment, for $\bar{N}_0 > \bar{N}_{0c}$, σ becomes a negative constant. The system is in a compressive state. When $M_0 \neq 0$ and after the buckling load, σ is not a constant and increases with \bar{N}_0 . It becomes positive for $\bar{N}_0 = 2414$, which means that from that point, the local stress repartition shows a tensile behaviour. At the end of the computed branch for which the buckled state corresponds to the experimental one, the residual stress value has the same order of magnitude as the measurement, for a beam width $b = 40 \text{ mm}$.

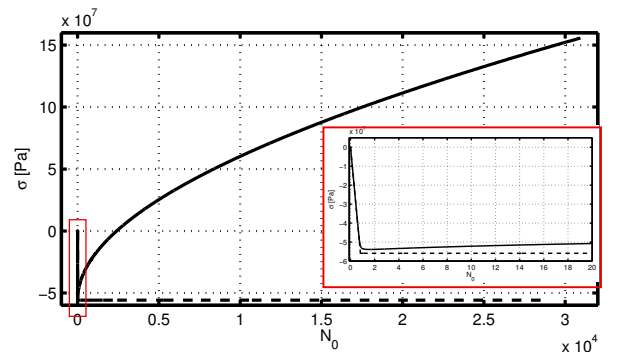


Figure 8: Residual stress evolution: (---) $\bar{N}_0 \neq 0$, $M_0 = 0$; (—) \bar{N}_0 and $M_0 \neq 0$

Finally, to quantify the residual stress and geometry effects, Eq. (15) is plotted with and without the residual stress terms (Fig. 9). We observe that before the beam buckled and for small deformation, in both cases ($M_0 = 0$ (Fig 9c) and $M_0 \neq 0$ (Fig 9d)), the residual terms decreases the eigenfrequencies values of about 15%. For $\bar{N}_0 > \bar{N}_{0c}$ and for large flexural deformations, the residual effect stays at a constant value when $M_0 = 0$ (Fig 9a) whereas when $M_0 \neq 0$ (Fig 9b), the gap between the eigenfrequencies computed with or without the residual stress increases continuously.

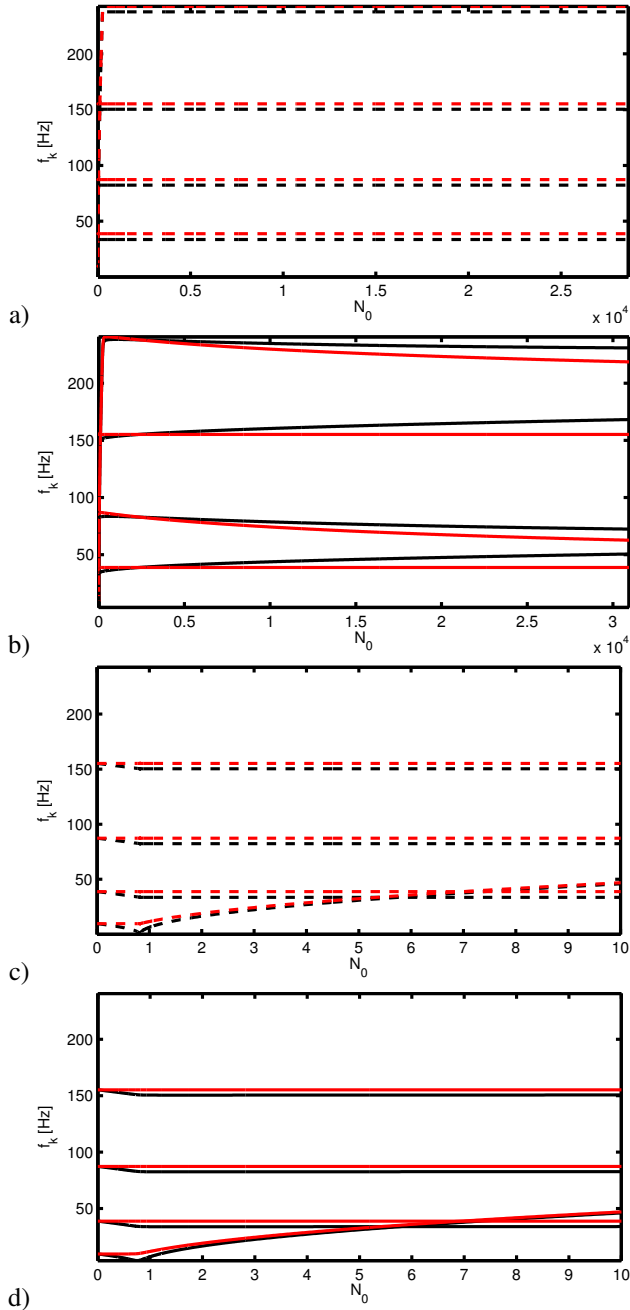


Figure 9: Impact of the residual stress state on the post-buckled eigenfrequencies : for all pictures (—) geometry only ; (---) geometry and residual stress terms. a) $\bar{N}_0 = [0 : 30000]$ and $M_0 = 0$; b) $\bar{N}_0 = [0 : 30000]$ and $M_0 = \bar{N}_0/10$. c) zoom of fig a: $\bar{N}_0 = [0 : 10]$ and $M_0 = 0$; d) zoom of fig b: $\bar{N}_0 = [0 : 10]$ and $M_0 = \bar{N}_0/10$

5 Conclusion and future work

In order to model the first step of the steelpan making, we have established a one-dimensional model of a prestressed buckled beam. We showed that experimental deformation is obtained when the initial stresses have two components: an axial force and a bending moment. Experimental tensile residual stress state is recovered. The eigenfrequencies of the buckled beam are mainly determined by the geometry with a residual stress state effect responsible of about 15% of their value, which is the main result of this work. This model will be expanded to circular plates with the aim of being closer to the real experimental process.

Acknowledgments

We thank to Emmanuel Judith, the *tuner*, who accepted to join us on this project of steelpan making study, and accepted to obey the rules of scientific research. We also thank Wilfrid Seiler from ENSAM, for the residual stress measurement realized by himself at his laboratory. The works presented in this paper have been supported by the DGA through a PhD grant.

References

- [1] A. Achong. The steelpan as a system of non-linear mode-localized oscillators, I: Theory, simulations, experiments and bifurcations. *Journal of Sound and Vibration*, 197(4):471–487, 1996.
- [2] A. Achong. Mode locking on the non-linear notes of the steelpan. *Journal of Sound and Vibration*, 266:193–197, 2003.
- [3] B. Cochelin and C. Vergez. A high order purely frequency-based harmonic balance formulation for continuation of periodic solutions. *Journal of Sound and Vibration*, 324:243–262, 2009.
- [4] D. Gay. Finite Element Modelling of Steelpan Acoustics. In *Acoustic2008*, 2008.
- [5] W. Huang. *Contribution à l'analyse par diffractométrie X des déformations et des contraintes à l'échelle des grains*. PhD thesis, Laboratoire d'Ingénierie des Matériaux, ENSAM, CER de Paris, 2007.
- [6] A. Lazarus and O. Thomas. A harmonic-based method for computing the stability of periodic solutions of dynamical systems. *C.R. mécanique*, 338:510–517, 2010.
- [7] F. Muddeen and B. Copeland. Sound radiation from Caribbean steelpans using nearfield acoustical holography. *Journal of the Acoustical Society of America*, 131(2):1558–1565, 2012.
- [8] L. E. Murr, E.V. Esquivel, Lawrie S.C., Lopez M.I., Lair S.L., K.F. Soto, S.M. Gaytan, D. Bujanda, R.G. Kerns, P.A. Guerrero, and J.A. Flores. Fabrication of aluminum, Caribbean-style, musical pan: Metallurgical and acoustical characterization. *Material Characterization*, 57:232–243, 2006.
- [9] A.H. Nayfeh. *Nonlinear Oscillations*. Wiley Classics Library, 1979.
- [10] T. D. Rossing and Hansen Uwe J. Vibrational mode shapes in Caribbean steelpans. II.cello and bass. *Applied acoustics*, 65:1233–1247, 2004.
- [11] T. D. Rossing, Hansen Uwe J., and D. S. Hampton. Vibrational mode shapes in Caribbean steelpans. I. Tenor and double second. *Journal of the acoustical society of america*, 108(2):803–812, 2000.